Progress in Additive Manufacturing (2023) 8:19–25
https://doi.org/10.1007/s40964-022-00384-6

FULL RESEARCH ARTICLE

Topology optimization for the design of a 3D-printed rotating shaft balance

Bram Noordman[1] · Yoeri Ton[1] · Jort van den Toorn[1] · Marc de Smit[1] · Ralph Haagsma[1] · Tim Koenis[1] · Wouter van den Brink[1]

Received: 13 December 2022 / Accepted: 22 December 2022 / Published online: 16 January 2023

Abstract
Rotating shaft balances (RSBs) are devices that are used to measure rotor blade forces and moments of wind tunnel models during wind tunnel tests. The design of an RSB can be challenging, because it has to comply with many and sometimes contradicting requirements such as high stiffness and high strain gauge bridge outputs. The manufacturing of a conventional RSB consists of different subsequent steps, which can be time consuming, expensive and associated with many risks. Therefore, in this work, the authors investigate if a RSB can be designed by topology optimization and manufactured by 3D printing. A topology optimization method was developed with as design objective the minimization of strain energy with constraints for the volume of the RSB's midsection, defined stresses at strain gauge locations used for the measurement of axial force and torque and an overhang constraint for additive manufacturing. The optimal preliminary design found by topology optimization was translated into a final printable design with the highest bridge sensitivity for axial force and torque, sufficient output for in-plane forces and moments and an acceptable safety factor on strength for combined loads. After adding extra supports required for printing, the RSB was successfully printed in metal by the laser powder bed fusion process, resulting in a product without external defects. The same topology optimization and manufacturing method can potentially be used for other balance types, leading to a reduction in total lead time and manufacturing costs while increasing the design freedom.

Keywords Topology optimization · Additive manufacturing · Strain gauge balances · L-PBF · Aerospace testing · Wind tunnel measurement

1 Introduction

In a wind tunnel test, the forces and moments on the model need to be measured accurately. A strain gauge balance is a high precision device that measures these loads during a test. A strain gauge balance typically consists of sets of flexures that are designed to deform under loads in different directions. Strain gauges are bonded to the flexures and electrically coupled in a Wheatstone bridge circuit to convert strain caused by deformation of the flexures under loading to bridge output voltages. With the balance calibration coefficients, this voltage is back-calculated to the loads acting on the model.

✉ Bram Noordman
Bram.Noordman@nlr.nl

[1] Royal Netherlands Aerospace Centre (NLR), Marknesse, The Netherlands

Various kinds of strain gauge balances exist, e.g., internal, external and Rotating Shaft Balances (RSBs). Internal balances are placed inside the wind tunnel model, between the model and the sting, and do not interfere with the flow, whereas external balances are placed outside the wind tunnel model. RSBs are used to measure loads on rotating blade structures and are most often placed inside or adjacent to the rotor hub.

1.1 Rotating shaft balance and application

An example of a 6-component RSB [1] designed by the Royal Netherlands Aerospace Centre (NLR) is shown in Fig. 1. It typically consists of two sets of four flexures instrumented with strain gauges and can measure three force components: axial, side and normal force and three moment components: rolling, pitching and yawing moment. Two of these RSBs were applied in each Contra-Rotating Open Rotor (CROR) engine of a concept Airbus T-tail aircraft

Fig. 1 Example of an NLR rotating shaft balance (left) with telemetry rotor (mid) and stator (right) [1]

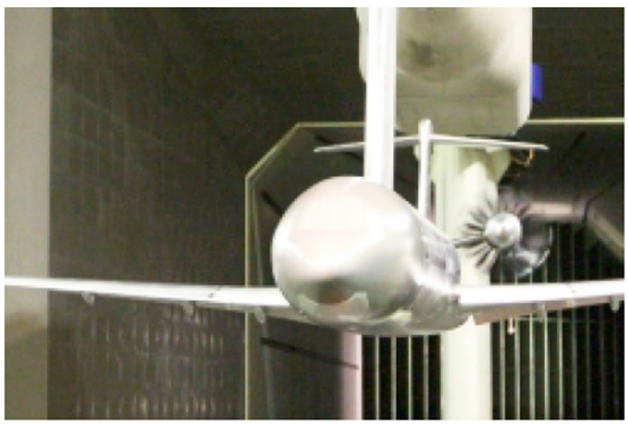

Fig. 2 Example of a Contra-Rotating Open Rotor engine application for NLR's rotating shaft balances on a concept Airbus T-tail aircraft model for a Clean Sky 2 EU program [1]

wind tunnel model, see Fig. 2, to investigate the CROR aeroacoustic performance at low speed test conditions.

1.2 Design optimization, manufacturing and instrumentation of a conventional RSB

The conventional NLR RSB design consists of an inner and outer ring with holes for interface bolts and dowel pins and two or sometimes three sets of four flexures depending on the magnitude of the loads and required balance stiffness. Flexure bending dimensions such as width, thickness and length are usually sized such that target strain gauge bridge outputs for single loads are obtained, a stiff balance design is achieved and safety factors on balance material yield strength are high enough for single and combined loads. Highest bridge sensitivities are desired for axial force and rolling moment and bridge outputs due to centrifugal load and any temperature gradient should be as low as possible. This is typically solved in a design optimization process with the use of a parametric finite element method (FEM) model, an example is the Half Model Balance (HMB) designed and produced by the NLR for the European Transonic Windtunnel (ETW) in Cologne [2]. Usually RSBs are manufactured from a high strength stainless steel and designed for infinite fatigue life. The fatigue life is determined for the final detailed design of the RSB together with the eigenfrequencies to avoid coincidence with rotational speeds in the operation region.

If the final detailed design of the RSB complies with all the requirements set by the customer and the ordered RSB material is received, the manufacturing can start. For a conventional RSB, the manufacturing consists of different subsequent steps like milling, turning, heat treatment, grinding, drilling of interface holes and Electrical Discharge Machining (EDM) of the flexures. After minimal surface grinding of the flexures, instrumentation of the flexures with strain gauges starts, usually followed by in-house calibration at room temperature with dead weights. Because the steps are sequential and more value is added in each step the process is time consuming, expensive and has an increasing risk the more work is put into the product. If something goes wrong in one of the steps, there is a risk that a step needs to be repeated if possible or the RSB needs to be fabricated again. Re-manufacturing can be faster with additive manufacturing.

1.3 Benefits of topology optimization and additive manufacturing of an RSB

In the context of the Clean Sky 2 JU Horizon 2020 project "Support to future CROR and UHBR Propulsion system Maturation (PropMat)", the authors investigate if a new type of RSB can be developed by topology optimization and Additive Manufacturing (AM). One advantage of using topology optimization for the design of the RSB is more design freedom. With topology optimization, we can find new and potentially stiffer designs compared to the traditional RSB design process where only the flexures of the RSB are optimized for high strain gauge bridge outputs. In addition, the weight of the RSB can be minimized quite easily with topology optimization if required.

Additive manufacturing of an RSB, also referred to as 3D printing, has an advantage that prototypes can be manufactured faster at lower costs compared to the traditional lengthy strain gauge balance manufacturing process, potentially leading to a reduction in total lead time and manufacturing costs [3]. Furthermore, several prototypes can be printed before manufacturing of the final RSB design, thereby reducing the likelihood of errors in the manufacturing process. Other advantages of additive manufacturing of an RSB compared to the traditional manufacturing process are potential energy savings using less machinery

and material waste reduction, because in the traditional RSB manufacturing process, a lot of material is removed; whereas in the AM process, only the material necessary to create the part is used. Of course, AM also comes with its own challenges like lower surface quality and dimensional accuracy, often requiring an extra process to achieve a certain surface finish or tolerance. The layering process of AM can also cause defects, so inspection is needed to check for defects.

2 Topology optimization method for a new RSB design

To optimize the design of an RSB in the pre-design phase by topology optimization, first, a suitable method had to be developed. In addition, a FEM model of the RSB is needed for this, which was created in SIMULIA Abaqus/CAE 2020 of Dassault Systèmes. The topology optimization was performed with SIMULIA Tosca Structure 2020.

2.1 Finite element model of the RSB

For the FEM model creation of the RSB, a base Computer-Aided Design (CAD) model of the RSB with a diameter of 126 mm was imported in Abaqus/CAE, consisting of two sets of four flexures with a waisted shape, an inner ring which is normally fitted on a shaft, an outer ring with bolt and dowel pin holes and a large midsection volume for topology optimization, which was created by partitioning the RSB geometry in Abaqus/CAE (see volume with color beige in Fig. 3).

The flexure front and side surfaces were partitioned to create strain gauge locations for strain gauge bridges BF_{xi} to measure output due to axial force F_x and BM_{xi} to measure output due to rolling moment M_x. These are considered the most important bridges for an RSB. Each bridge was carried out twice, which is normally done for an RSB to be redundant and compensate temperature effects. The strain gauge locations of bridge BF_{x1} are on the front faces of the horizontal flexures in Fig. 3 near the flexure roots and those of bridge BF_{x2} are on the vertical flexures near the roots. The strain gauge locations of bridge BM_{x1} are on the side surfaces of the front flexures near the root and those of bridge BM_{x2} are on the back flexures near the root. The RSB was meshed with 666,652 tetrahedral elements of type C3D4 in Abaqus. As boundary condition all the translational degrees of freedom (DOFs) were restrained at the shaft location. Typical RSB loads were taken:

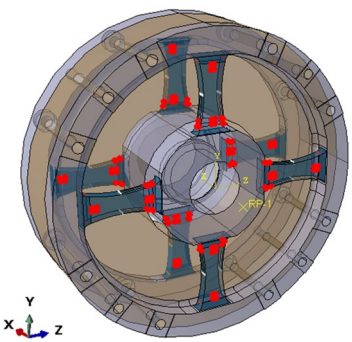

Fig. 3 Base geometry of RSB for topology optimization with strain gauge locations of all bridges in color red

- $F_x = 1300$ N,
- $F_y = F_z = 650$ N,
- $M_x = 160000$ N $*$ mm,
- $F_c = 6402$ RPM (centrifugal load).

The single force and moment loads were applied to a Reference Point (RP) in front of the RSB where normally the hub with blades is located. The applied force and moment loads are transferred to the RSB outer ring at the bolt and dowel pin locations with a continuum distributing coupling constraint. The dowel pins are mainly for the transfer of rolling moment and the bolt holes for other loads. As material for the RSB a stainless steel was chosen that can be printed with the Laser Powder Bed Fusion (L-PBF) process. The chosen material has a high stiffness, strength and fracture toughness. The material further has a small grain size and a relatively high hardness, which is beneficial for hysteresis. The Young's modulus of this material according to the material provider is 200 GPa with a Poisson's ratio of 0.278 and a density of 7700 kg/m^3. The yield strength of this material is 1600 MPa. The elastic properties were assigned to the RSB in the FEM model.

2.2 Topology optimization requirements

For the topology optimization of the RSB the following requirements were defined:

- The RSB design should be as stiff as possible, mass reduction was not directly of interest for a first prototype.
- In each Wheatstone bridge consisting of four strain gauges, two strain gauges should experience tensile stress and the other two compressive stress.
- Specific stress values are desired at the strain gauge locations of Wheatstone bridges BF_{x1}, $BF_{x2,}$ BM_{x1} and BM_{x2} for the single loads F_x and M_x.
- Low stress values are desired at the strain gauge locations of Wheatstone bridges BF_{x1}, $BF_{x2,}$ BM_{x1} and BM_{x2} for centrifugal F_c.
- An overhang angle constraint is needed for 3D printing of the RSB.

- The interface holes for bolts and dowel pins should be maintained.

2.3 Topology optimization method

The topology optimization requirements were translated into an objective and various constraints. The objective function was defined as the minimization of the strain energy of the RSB for the defined load cases F_x, F_y, F_z, M_x and F_c to achieve a stiff balance design. For the volume of the midsection of the RSB a constraint for volume (V) was defined as function of the initial volume (V_0): $V \leq 0.5 * V_0$. The stress outputs at the strain gauge locations of the Wheatstone bridges were constrained such that the bridge outputs in milliVolt (mV) are:

- 4 mV $\leq BF_{x1} \leq$ 6 mV for F_x,
- 4 mV $\leq BF_{x2} \leq$ 6 mV for F_x,
- 4 mV $\leq BM_{x1} \leq$ 6 mV for M_x,
- 4 mV $\leq BM_{x2} \leq$ 6 mV for M_x,
- $BF_{x1} \leq$ 0.5 mV for F_c,
- $BF_{x2} \leq$ 0.5 mV for F_c,
- $BM_{x1} \leq$ 0.5 mV for F_c,
- $BM_{x2} \leq$ 0.5 mV for F_c.

The Wheatstone bridge output constraints were translated to stress constraints with the Wheatstone bridge definition using a gage factor k of 2, bridge excitation voltage (V_{ex}) of 5 V and a Young's modulus of 200 GPa. As design variable for stress, the scaled centroidal von Mises stress was used, because the component stress was not available in SIMULIA Abaqus/CAE 2020 and Tosca Structure 2020. Component stress will be available in future versions through a user subroutine. This user subroutine was beta tested by the corresponding author after the PropMat project. The centroidal von Mises stress is equal to the von Mises stress in the flexures of the RSB, because these are outside the topology optimization domain and therefore, the element density in that region is not changed. For 3D printing of the RSB, an overhang angle was defined of 45° with respect to the global *x*-direction, which is the print direction. The bolt and dowel pin holes are part of the frozen design domain, hence the material density is not changed in this area.

3 Topology optimization and detailed design results

In the pre-design phase, an optimal material distribution was found for the midsection of the RSB by topology optimization in Tosca Structure 2020. The optimal RSB design found with topology optimization was subsequently translated into a final printable detailed design for additive manufacturing taking into account extra printability requirements not covered in the topology optimization.

3.1 Optimal design results

The optimal RSB material distribution found in terms of relative density (ρ/ρ_0) after 58 iterations is shown in Fig. 4 with ρ_0 the initial element density and ρ the current element density. For the topology optimization the Solid Isotropic Material with Penalization (SIMP) interpolation scheme [4] was used to relate element density with stiffness with a default penalty factor of 3. As a result of the optimization process material is distributed mainly around the load paths surrounding the inner ring of the RSB towards the outer ring near the bolt holes where the loads are introduced.

Only the stress values for Wheatstone bridges BF_{x1} and BF_{x2} for single load F_x were lower than the required 80 MPa to give an output of 4 mV, due to the chosen cross sectional flexure dimensions. However, these stress values were considered acceptable and fixable in the detailed design phase by slightly changing the flexure cross sectional dimensions. All other topology optimization constraints were satisfied. The von Mises stress in the RSB flexures due to the single load case F_x is shown in Fig. 5 and the component stress S22 is shown in Fig. 6. The flexures deform in a typical S-shape, giving the required tensile and compressive stresses for a Wheatstone bridge.

The von Mises stress at the strain gauge locations of bridge BM_{x1} and BM_{x2} due to the single load case M_x is between 80 and 120 MPa, which is sufficient to comply with the bridge output requirements for those bridges. The component stress S22 in the flexures due to load case M_x is given in Fig. 7 and shows the largest tensile and compressive stresses at the root of the flexures near the inner ring of the RSB. All von Mises stress values at the strain gauge locations of all Wheatstone bridges are lower than or equal to 10 MPa due to centrifugal load F_c, which satisfies the

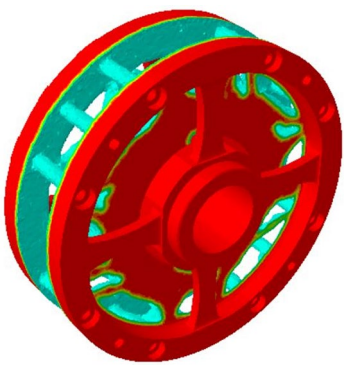

Fig. 4 Optimal RSB material distribution showing only relative densities (current/initial element density) of $\rho/\rho_0 \geq 0.3$ to filter 'hard' elements

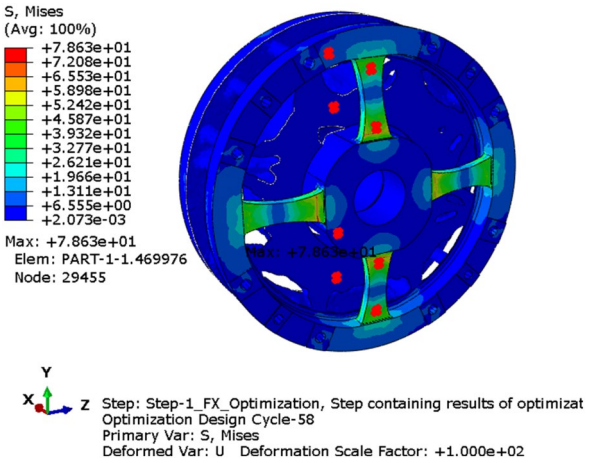

Fig. 5 Von Mises stress [MPa] in optimized RSB due to F_x with strain gauge locations of bridge BF_{x2} in color red

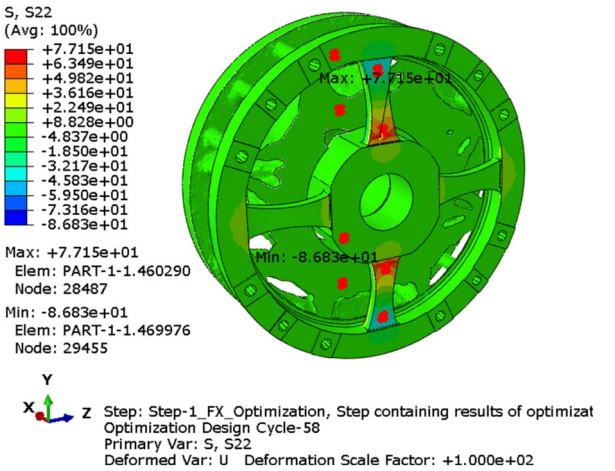

Fig. 6 Component stress S22 [MPa] in optimized RSB due to F_x with strain gauge locations of bridge BF_{x2} in color red

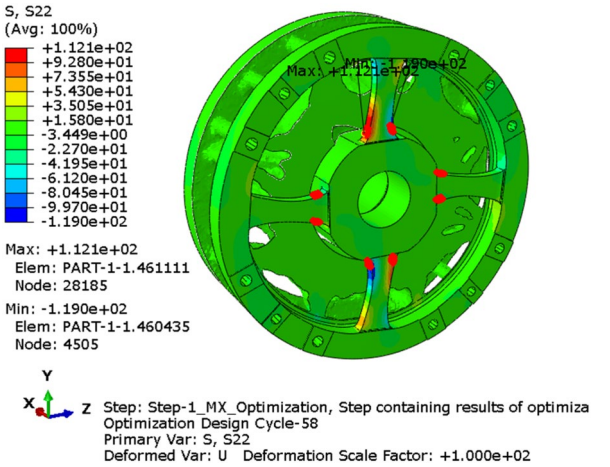

Fig. 7 Component stress S22 [MPa] in optimized RSB due to M_x with strain gauge locations of bridge BM_{x1} in color red

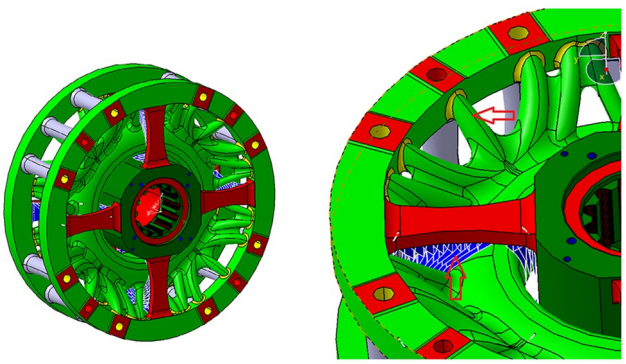

Fig. 8 Final detailed design of RSB in CATIA V5

required low bridge outputs for centrifugal load. The stresses in the flexures due to load cases F_y and F_z were also analyzed and gave lower values than for load case F_x. Likely, because the RSB was not optimized for those load cases.

3.2 Detailed design results

After an optimal RSB design was found by topology optimization, the printability was further investigated. In consultation with the engineers who manufacture the RSB, very thin supports were added between the front and aft flexures to enable 3D printing, see vertical arrow in the right picture of Fig. 8. Also connections were added to the outer ring near the dowel pin holes for extra stiffness at the dowel pin locations to resist the rolling moment (horizontal arrow in the right picture of Fig. 8). In addition, the flexure thickness and width were slightly decreased compared to the model for topology optimization to increase bridge outputs without having to repeat the topology optimization, the RSB diameter and total flexure length were kept the same.

As a final check before 3D printing of the RSB with the L-PBF process, the final design was analyzed in Abaqus to determine the stresses in the RSB due to single and combined loads and the bridge outputs due to single loads were determined. For this analysis the detailed CAD model of the RSB was imported in Abaqus/CAE and the RSB without supports for printing was meshed with 587,826 tetrahedral elements of type C3D10. The thin supports between the flexures were meshed with 17,216 shell elements of type S8R. The flexures of the RSB and supports were connected with shell-to-solid coupling constraints. For the boundary condition of the RSB all translational DOFs were restrained at the shaft location. In the detailed FEM model, strain gauge locations were added for all Wheatstone bridges of the 6-component RSB and 7 single

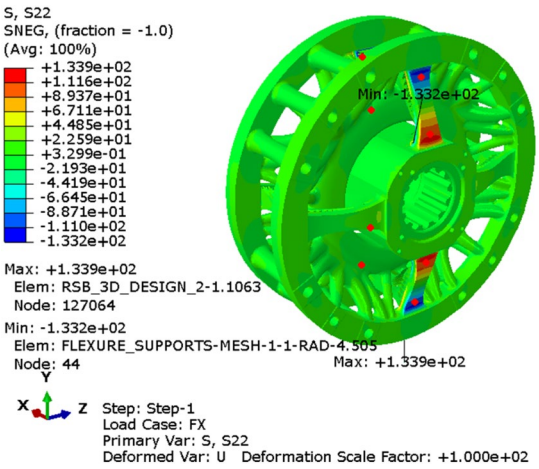

Fig. 9 Component stress S22 [MPa] in detailed RSB design due to F_x with strain gauge locations of bridge BF_{x2} in color red

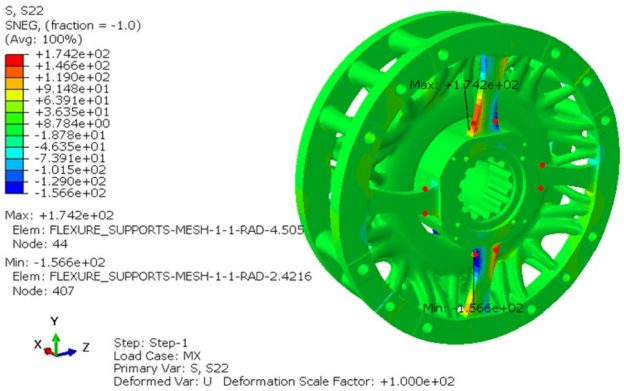

Fig. 10 Component stress S22 [MPa] in detailed RSB design due to M_x with strain gauge locations of bridge BM_{x1} in color red

loads were defined: F_x, F_y, F_z, M_x, M_y, M_z and centrifugal load F_c. The following typical RSB moments were added in addition to the loads already defined in the RSB model for topology optimization:

- $M_y = 120{,}000$ N*mm,
- $M_z = 120{,}000$ N*mm.

The moment loads were applied to a RP in front of the RSB. The moment loads are transferred to the RSB outer ring with a continuum distributing coupling constraint. The same stainless steel properties as used in the topology optimization were assigned to the whole RSB. The component stress S22 in the RSB flexures due to single loads F_x and M_x are shown in Figs. 9, 10, respectively. To increase the stresses in the flexures due to these load cases compared to the optimal design found with topology optimization, thinner and slightly less wide flexures were used in the detailed RSB design.

The calculated main bridge outputs for the detailed design of the RSB are shown in Table 1. The largest bridge outputs are for bridge BF_{x1} due to F_x and bridge BM_{x1} due to M_x for which the RSB was optimized. The outputs for bridges BM_{y1} and BM_{z1} due to moment M_y and M_z, respectively, are second largest. The lowest bridge outputs are for bridges BF_{y1} and BF_{z1} due to side force and normal force, respectively, but are still sufficiently high to measure in-plane blade forces. In conventional RSB designs, these bridge outputs are normally also the lowest and the largest bridge outputs are for axial force and rolling moment.

The combined load cases that an RSB can experience during wind tunnel testing were also evaluated for the detailed RSB design by linear combining the single load case results. Because each single load can have a positive and negative sign, $2^6 = 64$ combined load cases were postprocessed to find the most critical combined load case, which turned out to be load case $+F_x + F_y + F_z - M_x + M_y - M_z F_c$ with a maximum von Mises stress of 521 MPa at the root radius of a flexure. This gives a safety factor of 3.07 on the yield strength of the stainless steel, which is satisfactory to comply with wind tunnel model requirements.

3.3 Additive manufacturing results

The final design of the RSB was successfully printed at NLR's Metal Additive Manufacturing Technology Centre (MAMTeC) with the L-PBF process after optimization of L-PBF settings, resulting in a product with no surface defects. After printing, secondary manufacturing processes were applied, e.g., to remove material from the interfaces and flexures by milling to achieve tolerances and a low

Table 1 Calculated RSB main bridge outputs [mV] due to single loads for $V_{ex} = 5$ V and a gage factor of $k = 2$

	F_x	F_y	F_z	M_x	M_y	M_z
BFx_1	5.03	0.00	0.00	− 0.01	0.00	0.00
BFy_1	0.00	1.02	0.00	0.00	0.00	− 3.06
BFz_1	0.00	0.00	1.02	0.00	3.06	0.00
BMx_1	− 0.01	0.00	0.00	6.66	0.00	0.00
BMy_1	0.00	0.00	1.02	0.00	3.06	0.00
BMz_1	0.00	− 1.02	0.00	0.00	0.00	3.06

Fig. 11 Additively manufactured RSB

surface roughness for instrumentation, as can be seen in Fig. 11. Also, some block supports were removed between the flexures and midsection of the RSB. The lead time of the L-PBF process and secondary manufacturing processes was, respectively, 53 and 80 h. Secondary manufacturing process time might be slightly decreased if a new RSB topology can be found needing less supports that have to be removed. The next step will be instrumentation with strain gauges and calibration of the balance to demonstrate the technology readiness and validate the predicted performance by FEM.

4 Conclusions

In this paper, it has been shown that:

- A new design for an RSB can be developed with topology optimization complying with requirements for balance stiffness, bridge outputs and strength.
- The topology optimized RSB can be printed in stainless steel after optimization of L-PBF settings and adding extra supports between the front and aft flexures of the RSB for 3D printing.

Acknowledgements The PropMat project has received funding from the Clean Sky 2 Joint Undertaking under the European Union's Horizon 2020 research and innovation programme under grant agreement No 680954. The document reflects only the author's view; the JU is not responsible for any use made of the information contained herein.

Data Availability The datasets generated during and/or analysed during the current study are not publicly available due to confidentiality but are available from the corresponding author on reasonable request.

Declarations

Conflict of interest On behalf of all authors, the corresponding author states that there is no conflict of interest.

References

1. Bardet SM, Zwemmer R, Faasse PR, de Goede JI (2015) A contactless telemetry system for a contra-rotating open rotor test campaign, NLR-TP-2015–172 https://www.nlr.org/wp-content/uploads/2017/11/NLR-CRPDT-system.pdf
2. Wright MCN, Nahuis BR, Noordman BAT, Vankan WJ (2015) Design, manufacture and commissioning of a new NLR half model balance for ETW, 53rd AIAA Aerospace Sciences Meeting, pp 1–15
3. Burns DE, Parker PA (2020) Additively manufactured wind-tunnel balance. J Aircr 57(5):958–963
4. Sparlund J, Structural optimization of base engine component (2017) Master's thesis in Applied Mechanics. Chalmers University of Technology, Gothenburg, Sweden